

MODELING THE OUT-OF-PLANE BENDING BEHAVIOR OF RETROFITTED URM WALLS

J. I. Velázquez Dimas, Professor, Facultad de Ingeniería, Universidad Autónoma de Sinaloa, Mexico
M.R. Ehsani, Professor CEEM Department, The University of Arizona, Tucson, AZ
J. H. Castorena González, Professor, Esc. de Ing. Mochis, Universidad Autónoma de Sinaloa, Mexico
A. Reyes Salazar, Professor, Facultad de Ingeniería, Universidad Autónoma de Sinaloa, Mexico

Abstract

The classical laminated plate theory has been used to develop a simplified analytical model for predicting the out-of-plane behavior of URM wall retrofitted with glass fiber composites. The predictions of the model were compared with experimental results from reduced-scale wall tests. The correlation between the analytical model and experimental results was found to be very good.

Introduction

URM buildings constitute the main part of the buildings inventory worldwide. When subjected to seismic forces, the walls forming the structural system of this type of buildings experience the action of in-plane and out-of-plane forces. Failure modes related to both types of forces are characterized by a diagonal crack pattern and horizontal cracks along bed-joints as documented by many researchers [1,2].

Failure due to out-of-plane bending is recognized by the earthquake engineering community as the more dangerous [3,1], and attributes to structural damage and loss of life. Due to the advantages of composites materials with respect to conventional construction materials such as steel, they have been used in many applications to strength URM buildings to increase their in-plane and out-of-plane load-carrying capacity [4, 5, 6].

This paper presents the mathematical modeling of the flexural behavior of URM walls retrofitted with fiber composites using the Classical Laminated Plate Theory (CLPT). The walls analyzed are those subjected to uniform load and with boundary conditions defined by two sides free and the others two simple supported.

Background

There have been reported many studies about modeling the behavior of URM walls subjected to in-plane and out-of-plane loading [7, 8, 9]. However, little research has been done on mathematical modeling of URM walls retrofitted with composites and subjected to out-of-plane bending. Some such studies are discussed next. Schwegler [5], was the first to report a study where carbon fiber composite strips were used to retrofit one URM building. He tested wall panels under in-plane and out-of-plane loading and found that composite materials are a viable alternative to retrofit URM buildings to increase their strength and stiffness. He also developed an analytical model for in-plane behavior.

Triantafillou [10], conducted an experimental work on beams constructed with hollow clay bricks strengthened with composites strips. The main objective in that study was to investigate the effect of the reinforcement on the strength and the mode of failure of beams. From experimental results he

concluded that it is better to use composites strips bonded to the wall surface with spaces in between instead of covering the whole wall surface. He also developed an analytical model for beams retrofitted with composite strips and suggested the use of laminated plate theory for walls having composite reinforcement covering the whole surface.

Velázquez-Dimas and Ehsani [11], based on experimental results of seven half-scale brick masonry walls externally strengthened with vertical glass-fabric composite strips, and subjected to out-of-plane loading, developed an analytical model for predicting the flexural behavior of tested walls. The main parameters investigated were the amount of composites, the height-to-thickness ratio (h/t), the tensile strain in composites, and the mode of failure. According to the obtained results, they concluded that the behavior of the walls is best predicted with a linear elastic approach.

Modeling with CLPT

In this part, the Classical Laminated Plate Theory (CLPT) is used to develop the models for the investigated masonry walls. The behavior of the walls is divided into two stages that are: the stage corresponding to the first bed-joint crack and the stage corresponding to the ultimate load, for details see [12]. In order to differentiate both stages more clearly, the first one is called the symmetrical case and the second non-symmetrical. Therefore the mathematical work is done in two parts that are developed next.

Theoretical Concepts of CLPT

In this part, general concepts of CLPT that are important for this study are developed. First of all, the boundary conditions of the cases to be investigated are shown in Figure 1. It is important to say that only plates with two sides free and the other two simple supported will be analysed. This is because the available experimental data is for walls having such boundary conditions. In addition, a uniformly distributed load (q_0) is assumed to act on the surface of the wall parallel to the Z-axis.

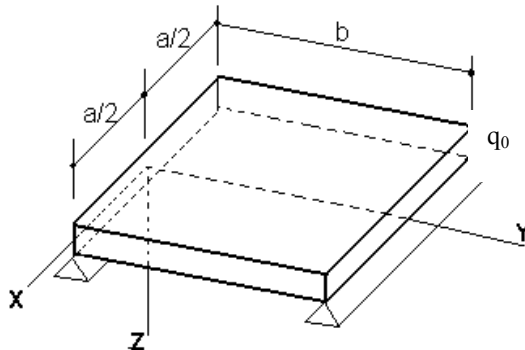


Figure 1. Reference system, boundary and loading conditions of the discussed model

The corresponding laminar arrangement of the studied walls is depicted in Figure 2. With this layer arrangement the theoretical work is simplified due to the symmetrical distribution of the layers. It is assumed that similar layers having the same thickness and fiber distribution are above and below the middle plane of the plate. Therefore, according to the CLPT the components B_{ij} of the constitutive equations are zero.

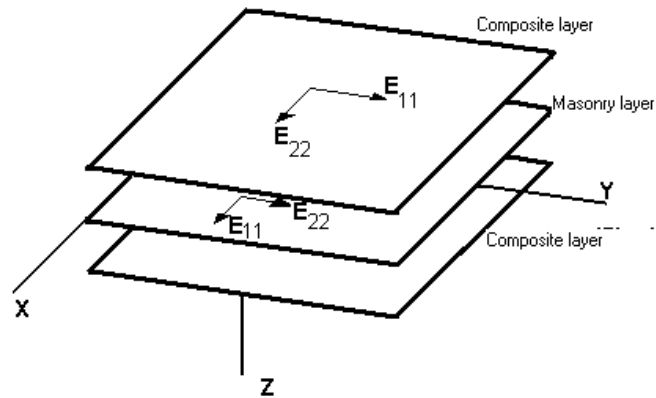


Figure 2. Coordinate system and layer arrangement $[90^\circ/0^\circ/0^\circ/90^\circ]$ for a typical wall

Analysis of symmetrical laminated plate

For analysis of this type of plates, many theories have been developed and they can be linear and nonlinear. Also Finite Element Method has been widely used for analysis of laminated plates. According to the geometry properties, the plates can be thin or thick ones, and symmetrical and nonsymmetrical. However, the approach based on thin plates is the most common for doing analysis since the shear and transverse normal strains are not considered. Therefore, in this study the CLPT is used for a thin plate. In order to apply this approach the following assumptions are taken into account [12].

1. Each plate is composed of an arbitrary number of layers perfectly bonded such that no relative displacement takes place.
2. Each layer is homogeneous, orthotropic and behaves elastically.
3. The plate thickness is small with respect to its other dimensions.
4. The displacement components u , v and w are small compared with the plate thickness.
5. Each ply is of uniform thickness.
6. Transverse shear strains are zero.
7. Transverse normal strain is zero.
8. Body forces are neglected.
9. The displacement u and v are linear function of z .

Assumptions 6 and 7 are called Kirchhoff assumptions and the problem can be reduced to a two dimensional study of the middle plane. Combining equilibrium, displacements and strain equations with the latter assumptions, the constitutive relationships for laminated plates can be developed. Such equations are shown next:

$$\begin{bmatrix} N_x \\ N_y \\ N_{xy} \\ M_x \\ M_y \\ M_{xy} \end{bmatrix} = \begin{bmatrix} A_{11} & A_{12} & A_{16} & B_{11} & B_{12} & B_{16} \\ A_{11} & A_{22} & A_{26} & B_{12} & B_{22} & B_{26} \\ A_{16} & A_{26} & A_{66} & B_{16} & B_{26} & B_{66} \\ B_{11} & B_{12} & B_{16} & D_{11} & D_{12} & D_{16} \\ B_{12} & B_{22} & B_{26} & D_{12} & D_{22} & D_{26} \\ B_{16} & B_{26} & B_{66} & D_{16} & D_{26} & D_{66} \end{bmatrix} \begin{bmatrix} \varepsilon_x \\ \varepsilon_y \\ \varepsilon_{xy} \\ \kappa_x \\ \kappa_y \\ \kappa_{xy} \end{bmatrix} \quad (1)$$

Where A_{ij} is called extensional stiffness, D_{ij} the bending stiffness, and B_{ij} the bending-extensional coupling stiffness [13], which are defined in terms of the lamina stiffness $Q^{(k)}_{ij}$ and the plate thickness h , and the coordinate z as:

$$(A_{ij}, B_{ij}, D_{ij}) = \int_{-h/2}^{h/2} (1, z, z^2) Q^{(k)}_{ij} dz \quad i, j = 1, 2, 6 \quad (2)$$

Taking into account the layer arrangement shown in Figure 2, the force vector of (2) is divided in two parts which are the stress resultant and moment resultant equation. It is important to say that a non-coupling system is obtained where the extension is independent of bending. Furthermore, the differential equation for a symmetric and orthotropic laminated plate with no inertial terms is given as [12]:

$$D_{11} \frac{\partial^4 w}{\partial x^4} + 2(D_{12} + 2D_{66}) \frac{\partial^4 w}{\partial x^2 \partial y^2} + D_{22} \frac{\partial^4 w}{\partial y^4} = q_0 \quad (3)$$

Analytical Solution

In order to solve Eq. (3), many solutions are available. However, in this study an approach suggested by Levy [12, 14] is used. This approach was chosen because allows solutions for plates having boundary conditions with two sides free and the other two simple supported, i.e. similar to the walls tested in the available experimental studies. For solving Eq. (3) Levy suggested the following displacement function.

$$w_{(x,y)} = w_{0(y)} + w_{1(x,y)} \quad (4)$$

Where each term is given by:

$$w_0(y) = \frac{4b^4 q_0}{D_{22} \pi^5} \sum_{n=1}^{\infty} \frac{1}{n^5} \sin \frac{n \pi y}{b} \quad (5)$$

$$w_1(x, y) = \sum_{n=1}^{\infty} X_n(x) \sin \frac{n \pi y}{b} \quad (6)$$

Ashton and Whitney[12], have solution for plates with boundary conditions denoted by two sides simple supported and two fixed. However, for the case discussed in this study no reference was found for a solution. The full development of such solution can be found in [15]. Due to the fact that the solution requires many time consuming steps its development is not shown in this study. According to the solution given by Eq. (4) and the boundary conditions to be satisfied, the following equation can be obtained:

$$q_0 + \sum_{n=1,3,5,\dots}^{\infty} \left[D_{11} X_n'''' - 2(D_{12} + 2D_{66}) \left(\frac{n\pi}{b} \right)^2 X_n'' + D_{22} \left(\frac{n\pi}{b} \right)^4 X_n(x) \right] \text{sen} \left(\frac{n\pi}{b} \right) = q_0 \quad (7)$$

where the prime denotes differentiation with respect to x. Thus the function $X_n(x)$ must satisfy the homogeneous equation.

$$D_{11} X_n'''' - 2(D_{12} + 2D_{66}) \left(\frac{n\pi}{b} \right)^2 X_n'' + D_{22} \left(\frac{n\pi}{b} \right)^4 X_n(x) = 0 \quad (8)$$

The general solution of Eq. (8) can be written in terms of four arbitrary constants A_n, B_n, C_n and D_n . The particular form of the solution depends upon the roots of the characteristic Eq. (9):

$$D_{11} s^4 - 2(D_{12} + 2D_{66}) s^2 + D_{22} = 0 \quad (9)$$

Three solutions exist for Eq. (9), which are:

Case 1: The roots are real and unequal and denoted by $\pm s_1$ and $\pm s_2$ ($s_1, s_2 > 0$). This solution can be written as:

$$w = \sum_{n=1,3,5,\dots}^{\infty} \left[\frac{4b^4 q_0}{D_{22} \pi^5} \frac{1}{n^5} + A_n \cos \alpha \cosh \gamma + D_n \sin \alpha \sinh \gamma \right] \sin \frac{n \pi y}{b}$$

$$w = \sum_{n=1,3,5,\dots}^{\infty} \left[\frac{4b^4 q_0}{D_{22} \pi^5} \frac{1}{n^5} + \frac{D_{12}}{D_{22}} \frac{4b^4 q_0}{\pi^5} \frac{1}{n^5} \frac{\varepsilon_4}{\varepsilon_3 \varepsilon_2 - \varepsilon_1 \varepsilon_4} \cos \alpha \cosh \gamma \right. \\ \left. + \frac{D_{12}}{D_{22}} \frac{4b^4 q_0}{\pi^5} \frac{1}{n^5} \frac{\varepsilon_3}{\varepsilon_1 \varepsilon_4 - \varepsilon_2 \varepsilon_3} \sin \alpha \sinh \gamma \right] \sin \frac{n \pi y}{b} \quad (10)$$

Case 2: The roots are real and equal and denoted by $\pm s$ ($s > 0$). This solution can be written as:

$$\begin{aligned}
 w &= \sum_{n=1,3,5,\dots}^{\infty} \left[\frac{4b^4 q_0}{D_{22} \pi^5} \frac{1}{n^5} + A_n \cosh \alpha_1 + C_n \cosh \alpha_2 \right] \sin \frac{n\pi y}{b} \\
 w &= \sum_{n=1,3,5,\dots}^{\infty} \left[\frac{4b^4 q_0}{D_{22} \pi^5} \frac{1}{n^5} + \frac{D_{12}}{D_{22}} \frac{4b^4 q_0}{\pi^5} \frac{1}{n^5} \frac{K_2}{\Delta_n^1} \sinh \alpha_4 \cosh \alpha_1 \right. \\
 &\quad \left. - \frac{D_{12}}{D_{22}} \frac{4b^4 q_0}{\pi^5} \frac{1}{n^5} \frac{K_1}{\Delta_n^1} \sinh \alpha_3 \cosh \alpha_2 \right] \sin \frac{n\pi y}{b}
 \end{aligned} \tag{11}$$

Case 3: The roots are complex and denoted by $s \pm ti$ and $-s \pm ti$ ($s, t > 0$), and written as:

$$\begin{aligned}
 w &= \sum_{n=1,3,5,\dots}^{\infty} \left[\frac{4b^4 q_0}{D_{22} \pi^5} \frac{1}{n^5} + A_n \cosh \alpha_5 + D_n x \sinh \alpha_5 \right] \sin \frac{n\pi y}{b} \\
 w &= \sum_{n=1,3,5,\dots}^{\infty} \left[\frac{4b^4 q_0}{D_{22} \pi^5} \frac{1}{n^5} + \frac{D_{12}}{D_{22}} \frac{4b^4 q_0}{\pi^5} \frac{1}{n^5} \frac{n\pi}{b} \left(\frac{2\xi_3}{\xi_1 \xi_4 - \xi_2 \xi_3} \right) \cosh \alpha_5 \right. \\
 &\quad \left. + \frac{D_{12}}{D_{22}} \frac{4b^4 q_0}{\pi^5} \frac{1}{n^5} \frac{n\pi}{b} \left(\frac{2\xi_1}{\xi_3 \xi_2 - \xi_1 \xi_4} \right) x \sinh \alpha_5 \right] \sin \frac{n\pi y}{b}
 \end{aligned} \tag{12}$$

The last three equations are solutions based on an approach suggested by Levy. The Levy approach assumes a displacement function consisting of two parts which are: cylindrical flexure on a unit strip parallel to the “Y” axis and the other is the flexure parallel to “X”. Since the developed solutions are not easy for practical purposes, a simplified solution is developed next and this is the main objective of this study.

The simplified solution is obtained by considering only the cylindrical bending. With such models, displacements and load carrying capacity of URM retrofitted with fiber composites, and modeled with CLPT, can be predicted.

Symmetrical Case

This case corresponds to a wall that has no cracks. As pointed out at the beginning of this study, the behavior of the investigated walls is divided in two stages corresponding to the uncracked and cracked ones. Since many steps are involved in to develop the simplified model, in this paper only the final model is presented. However, it is important to say that the model is derived by keeping the first term of Eqs. (4) and (5), and by simplifying the equations due the symmetrical arrangement of the plate, and by assuming that $E_{11m} \cong 1.5E_{22m}$ [16] and $E_{11f} \cong 10E_{22f}$. Thus, the resulting simplified equation for displacements is given by Eq. (13).

$$w = \frac{3}{48 K_T} (y^4 - 2by^3 + b^3 y) q_0 \quad (13)$$

$$K_T = K_{re\ inf} + K_{wall}$$

$$K_{re\ inf} = \frac{n W_f}{a} \frac{E_{11} f}{1 - \frac{\nu_{12}^2}{10}} \left(\frac{h^3}{8} - \frac{h_m^3}{8} \right), \quad K_{wall} = \frac{E_{22} m}{1 - \frac{\nu_{12}^2}{1.5}} \frac{h_m^3}{8}$$

In addition, an expression for calculating the load corresponding to the rupture is developed and given by Eq. (14)

$$\sigma_y = \sigma_{rup} = - \frac{E_{22} m}{1 - \frac{\nu_{12}^2}{1.5}} \frac{h_m}{2} \frac{(y-b)y}{\frac{4}{3} [K_{reinf} + K_{wall}]} q_0 \quad (14)$$

where K_{reinf} and K_{wall} are defined in Eq. (13).

In order to get q_0 , the value of modulus of rupture $f_r = \sigma_{rup} = 2\sqrt{f'_m}$ (psi) (UBC-97) is given in Eq. (14). So the point corresponding to maximum tensile stress is obtained by using Eqs. (13) and (14)

Nonsymmetrical Case

As done in the previous case, a simplified mathematical model for a cracked behavior was developed. For this situation many mathematical developments were made. Due to space limitations, only general steps are herein described. The layer distribution showing the cracked and uncracked areas is depicted in Figure 3a, and the stress distribution is shown in Fig. 3b. In addition, a linear strain distribution across the wall section is assumed.

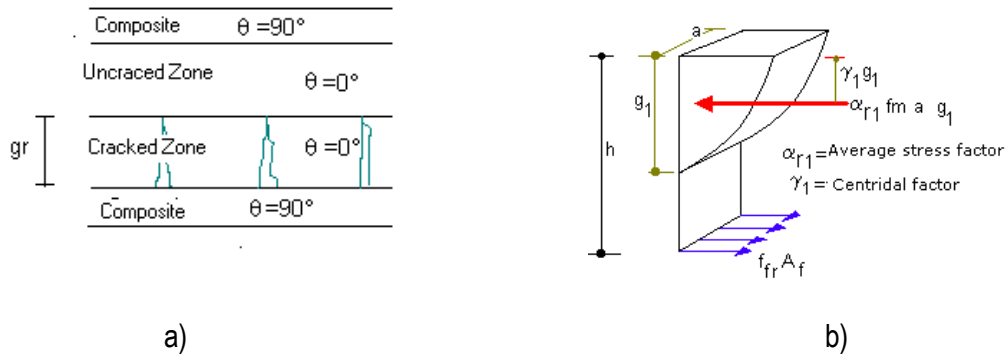


Figure 3. Cracked cross sectional and stress distribution

It is important to say that bending stresses in brick masonry through the plate thickness (h) were calculated based on a model proposed by [17], and the factors γ_1 and α_{r1} in model proposed by [18]. By using a statistical study of experimental available data, an averages values of $\alpha_{r1}=0.6025$ and $\gamma_1=0.3631$, were determined [15]. Thus, by taking into account the effect of delamination of composite strips on reducing the ultimate load-carrying capacity and to increase the deflection capacity, two models for ultimate load (q_{ult}) and ultimate deflection (W_{ult}) were developed. The corresponding mathematical expressions are:

$$q_{ult} = q_{max}(2.5\omega^{0.467}) \quad (15)$$

$$w_{max} = \frac{q_{ult}}{24D}(y^4 - 2by^3 + b^3y) \quad (16)$$

$$w_{ult} = \frac{w_{max}}{0.091\ln[\omega(\frac{b}{h})^2] + 0.2175} \quad (17)$$

Where composite reinforcement index ω , and q_{max} are given by:

$$\omega = 0.005 \frac{E_{11f}}{f'_m} \rho_v \quad (18)$$

$$q_{max} = \frac{8}{b^2} \frac{M_{resist}}{a} = \frac{8}{b^2} \frac{1}{2} f'_m h^2 \left\{ 0.6025 \left(\frac{g_1}{h} \right) [1 - 0.4375 \left(\frac{g_1}{h} \right)] + \frac{\omega}{\left(\frac{g_1}{h} \right)} \left(1 - \frac{g_1}{h} \right) \right\} \quad (19)$$

Application of the Proposed Equations

The mathematical models developed were used to estimate the experimental results of seven half-scale URM walls retrofitted with glass-fiber composite strip reported by [19, and 20]. The set of tested walls was divided into two sets which are corresponding to short walls and slender walls. All specimens were subjected to the same standard history pattern of static cyclic out-of-plane loading applied with an air-bag system. The specimens were simple supported at top and bottom and remained free along the vertical edges. The walls were 1220 mm (48 in.) wide and 50 mm (1.92 in.) thick. The small-scale bricks were cut from solid clay bricks and had a dimension of 102x49x38 mm (4.0x1.92x1.5 in.). Type N mortar similar to that used in old masonry buildings was used by the mason to construct the walls. Each set of walls had a different height. The slender walls were 1420 mm (56 in.) high (i.e. h/t=28) and the short walls were 710 mm (28 in.) high (i.e. h/t=14).

Two walls were selected for the purposes of validating the proposed simplified model for predicting their behavior. One wall is short one having aspect ratio h/t = 14 and reinforced with composite strips equivalent to 75% of the corresponding balanced condition (ρ_b). The other wall is a slender one with h/t = 28 and retrofitted with a composite reinforcement ratio equal to 100% the corresponding balanced condition (ρ_b). The results are shown in Figs. 4 and 5. As can be observed from both graphs, the predicted ones are very close to the experimental curves.

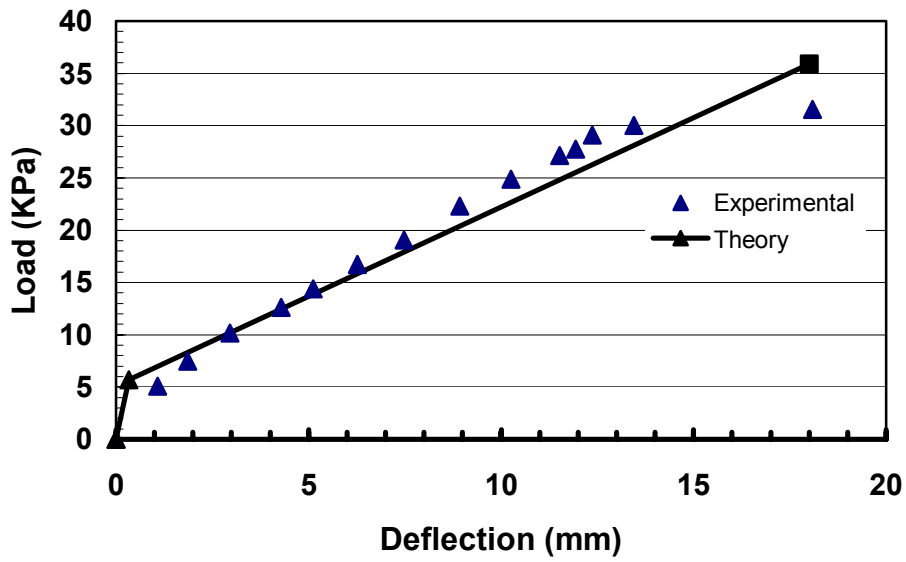


Figure 4. Theoretical and experimental graphs of a wall with $h/t = 14$ and $\rho = 0.75\rho_b$

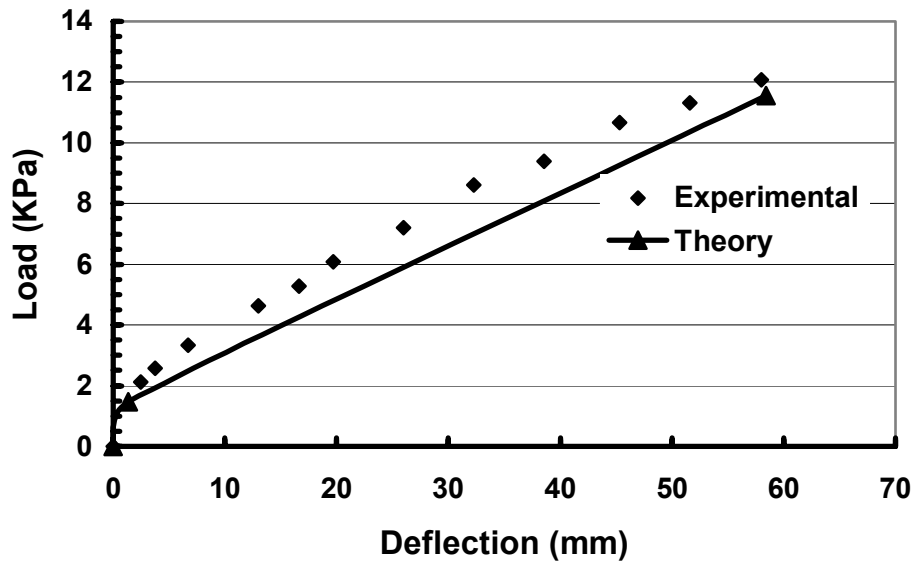


Figure 5. Theoretical and experimental graphs of a wall with $h/t = 28$ and $\rho = \rho_b$

Conclusions

Based on Classical Laminated Plate Theory and using an approach suggested by Levy, a simplified mathematical model that allows the estimation of points corresponding to the cracking and ultimate points of the load-deflection curves for URM walls retrofitted with FRP materials was developed.

From calculated values and comparison to available experimental data, it can be concluded that good correlation exists between both results

References

- [1] Bruneau, M. (1994), "State-of-the-art report on seismic performance of unreinforced masonry buildings." *ASCE Journal of Struc. Engineering.*, Vol.120, No. 1:230-251
- [2] Kehoe, B.E. (1996), "Performance of retrofitted unreinforced masonry buildings." paper No. 1417, *Eleventh World Conference on Earthquake Engineering*, Acapulco, Mexico.
- [3] Prawel, S.P. and Reinhorn, A.M. (1985), "Seismic retrofit of structural masonry using a ferrocement overlay." *Proceedings Third North-American Masonry Conference*. University of Texas at Arlington, 59.2-59.19.
- [4] Saadatmanesh, H and Ehsani, M.R. (1998). "Fiber Composites in Infrastructure," *Proceedings of the Second International Conference on Composites in Infrastructure*, Tucson, Arizona, Vols. I and II, USA
- [5] Schwgler, G.(1995), "Masonry Construction Strengthened with Fiber Composites in Seismically Endangered Zones". *10th European Conference In Earthquake Engineering*.
- [6] El-Badry, M.M. (1996), "Advanced Composites Materials in Bridges and Structures", *Proceedings ACMBS II*, Montreal, CA, 1027 pp.
- [7] Sinha, B.P. (1978). "A simplified ultimate load analysis of laterally loaded model orthotropic brickwork panels of low tensile strength," *The Structural Engineer*, 4(56B), pp. 81-84.
- [8] Dawe, J. L. and Seah, C.K. (1989). "Out-of-plane resistance of concrete masonry infilled panels," *Canadian Journal of Civil Engineering*, Vol.16, pp. 854-864.
- [9] Abrams, D.P., Angel, R. and Uzarski (1993). "Transverse strength of damaged URM infills," 6th North American Masonry Conference, Drexel University, PA.
- [10] Triantafillou, T.C.(1998), "Strengthening of Masonry Structures Using Epoxy-Bonded FRP Laminates". *Journal of Composites for Construction*, Vol.2, No.2.
- [11] Velazquez-Dimas, J.I, Ehsani, M. R., and Saadatmanesh, H. (2000). "Modeling Out-of-Plane Behavior of URM Walls Retrofitted with Fiber Composites," *ASCE Journal of Composites for Construction*, 4(4), 172-181.

- [12] Ashton, J.E., Whitney, J.M. (1970) "Theory of Laminated Plated". *Progress in Materials Science Series*, vol.IV.
- [13] Reddy, J.N (1997) "Mechanics of Laminated Composite Plates: Theory and Applications" CRC Press, 773 pp.
- [14] Reddy, J.N., Khdeir, A.A.(1987) "Lévy Type Solutions for Symmetrically Laminated Rectangular Plates Using First-Order Shear Deformation Theory". *Journal of Applied Mechanics*, No.54, 740-742 ,
- [15] Castorena Gonzalez, J.H. (2000) "Modelación Mediante la Teoría de Placas Laminadas de Muros de Mampostería Reforzados con Materiales Compuestos y Sujetos a Flexión" *Tesis de Maestría*, Facultad de Ingeniería de la Universidad Autónoma de Sinaloa.
- [16] Hendry, A. W., (1973) "The Lateral Strength of Unreinforced Brickwork", *The Structural Engineer*, V 51, pp. 43-50.
- [17] Turkstra, C. J. (1970) "Resistencia de Muros de Mampostería Ante Cargas Verticales Excentricas", Instituto de Ingeniería, Revista No. 274, UNAM, Mexico.
- [18] Park, R y Paulay, T., (1979) "Estructuras de Concreto Reforzado", Editorial Limusa, México.
- [19] Ehsani, M. R., Saadatmanesh, H. and Velazquez-Dimas, J.I. (1999), "Behavior of Retrofitted URM Walls Under Simulated Earthquake Loading", *ASCE Journal of Composite for Construction*, Vol. 3, No. 3: 134-142.
- [20] Velazquez-Dimas, J.I., Ehsani, M.R. and Saadatmanesh, H.(2000), "Out-of-Plane Bhavior of Brick Masonry Walls Strengthened with Fiber Composites". *ACI Structural Journal*, Vol.9 , No.3 377-387.

Notation

E_{11}	Modulus of elasticity of composite layer in principal (1) direction;
E_{22}	Modulus of elasticity of composite layer in transverse(2) direction;
ν_{ij}	Poisson ratio in the j-direction when a load is applied in the i-direction;
G_{ij}	Shear modulus;
κ_x	Plate curvature parallel to the xz-plane;
κ_y	Plate curvature parallel to the yz-plane;
κ_{xy}	Torsion of the plate surface along the x e y-axis;
a	Side length of the plate parallel to the x-axis;
b	Side length of the plate parallel to the y-axis;
N_x	Force per unit length parallel to the x-axis (side a);
N_y	Force per unit length parallel to the y-axis (side b)
N_{xy}	Shear resultant force per unit length;
M_x	Flexural Moment per unit length around Y-axis;
M_y	Flexural Moment per unit length around X-axis;

M_{xy}	Torsion Moment per unit length;
ε_x^0	Strain parallel to the x-axis of the plate middle plane;
ε_y^0	Strain parallel to the y-axis of the plate middle plane;
ε_{xy}^0	Shear strain of the plate middle plane.
z_k	Distance in z-direction from the middle plate surface to the layer k;
s	Real root or real part of a complex root;
t	imaginary part of a complex root;
α'	$=n\pi a/2b$
γ'	$=n\pi s a/2b$
α_1	$=n\pi s_1 x/b$
α_2	$=n\pi s_2 x/b$
α_3	$=n\pi s_1 a/2b$
α_4	$=n\pi s_2 a/2b$
u^0	Middle plane displacement of the plate in the X-direction;
v^0	Middle plane displacement of the plate in the Y-direction;
E_{22m}	Modulus of Elasticity perpendicular to bed-joint;
E_{11m}	Modulus of elasticity perpendicular to the brick head joints $E_{11m} > E_{22m}$
E_{11f}	Modulus of Elasticity parallel to the fiber orientation;.
E_{22f}	Transverse modulus of composite $E_{11f} \gg E_{22f}$;
E'_{11f}	$=n_1 W_f/a$
E'_{22f}	$=0.10E'_{11f}$
n_1	Number of composite strips bonded to the wall surface;
W_f	Wide of the composite strip;
h_m	Wall thickness
h'_m	$=h_m/2$
h_f	Thickness of composite strip;
h_t	$=h_m+2h_f$
gr	Depth of the cracked zone;
θ	Main fiber orientation measured with respect to principal axis plate;
g_1	Neutral axis depth on cracked walls;
h	Distance from top wall surface to the composite strip;.
M_{resist}	Nominal moment capacity of reinforced masonry;
f_m	Compression stress on brick masonry;
ε_m	Strain on brick masonry;
f_{fr}	Tension stress on composite strip;
A_f	Tensile composite reinforcement area;
ρ_v	$=A_f/ah$
ω	$=(\varepsilon_m E_{11f} f_m) \rho_v$
E_0	Modulus of elasticity calculated on straight part of the σ - ε curve
ε_0	Strain at maximum stress on masonry;
f_m	Compressive strength of masonry specimens;
ε_f	Strain on fiber